Comparative study of electron fluxes, ionization rates, ion and electron densities due to photoelectron and magnetospheric electron interaction with the atmosphere of Mars

S. A. Haider

Physical Research Laboratory, Ahmedabad 380 009, India

A comparative study of nighttime and daytime ionosphere of Mars has been made by calculating electron fluxes, ion production rates and ion and electron densities for the nightside and dayside ionosphere of Mars. For the calculation of nightside ionospheric study we have used the primary electron spectra measured by HARP experiment onboard the PHOBOS-2 martian orbiter. Calculations for monoenergetic (unit flux) ion production rates in the nightside have also been carried out. Analytical yield spectrum approach and coupled continuity equations for chemical steady-state conditions have been used to carry out this calculation. The electron densities calculated for daytime and nighttime are compared with the data of Viking 1 and 2 radio occultations respectively. It is found that the energy of electron spectra (few hundred eV) observed by HARP experiment in martian magnetosphere is sufficient for impact ionization of planetary neutral gas and characteristic flux could produce the nightside ionospheric layer with a peak density of a few thousands of electrons per cubic centimeter, which corresponds to densities earlier observed by the radio occultation experiment of Viking 2. The electron density for nighttime is found to be 20 times less than that of daytime and peaks at 30 km above the daytime ionosphere.

RADIO occultation measurements of electron density profiles in Martian ionosphere have been reported to start from the encounter of Mariner 4[1, 2], Mariner 6 and 7[3], Mars 2[4, 5], Mariner 9[6, 7], Mars 4, 5 and 6[8, 9] and Viking 1 and 2[10]. Unfortunately, only limited data are available in the nightside ionosphere of Mars from these missions. Few ionospheric profiles in the nighttime have been reported by Savich and Samovol[9], Lindal *et al.*[11] and Zhang *et al.*[12]. Recently, we have calculated[13, 14] the electron density and airglow emissions in the nighttime ionosphere of Mars using two different electron spectra[15] observed by Hyperbolic Analyser in Retarding Potential (HARP) experiment onboard PHOBOS-2 martian orbiter in magnetosphere and plasmasheet regions during second elliptical orbit. We have found that the characteristic energy of these electron spectra was sufficient for impact ionization with neutral species of the martian atmosphere.

In the present article we focus our attention primarily on a comparative study of nightside and dayside ionosphere of Mars. For this purpose we made a detailed study of the following aspects in the martian ionosphere: (i) secondary electron fluxes using magnetotail electron spectra[5] observed by HARP electron spectrometer during second elliptical orbit of PHOBOS-2 in the nightside, (ii) photoelectron flux, (iii) ion production rates, (iv) ion density, and (v) electron density for nightside and dayside. The calculated electron density profiles are compared with observations from Viking mission.

Input data

During *in situ* measurements onboard PHOBOS-2 martian orbiter, the electron fluxes were measured by HARP electron experiment within the energy range of 3–480 eV in eight angular sectors arranged symmetrically relative to the antisolar direction. In Figure 1 of our previous paper[13] we have shown the position of second elliptical orbit of PHOBOS-2 when the magnetotail electron spectra were measured[13]. Figures 2 and 3 of this paper show the magnetotail electron spectra measured on 5 February 1989 in the magnetosphere of Mars. This electron spectra is used in the present calculation of secondary electron flux in the nightside ionosphere of Mars. For the calculation of secondary electron flux at different altitudes above the nightside of Mars we should assume that electron flux measured by PHOBOS-2 is finally reaching lower heights down to the planetary atmosphere along the magnetic field lines. Due to lack of observational information on a real topology of areomagnetic field (e.g. whether it is mainly

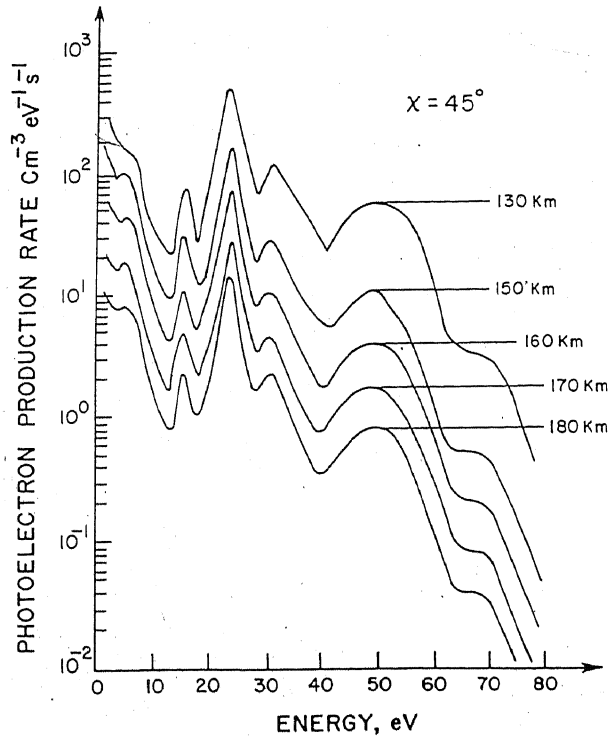

Figure 1. Photoelectron production rates at selected altitudes for $\chi = 45°$.

intrinsic or induced, which region of the planet is the observational point magnetically connected with, etc.) we will assume that local magnetic field inclination is 90°.

For the present calculations we have adapted the dayside model atmosphere of Mars given by Mantas and Hanson[16] for four gases CO_2, N_2, O_2 and O. Densities of minor constituents CO, NO and Ar were adopted from Fox and Dalgarno[17] profiles. In the height range of 150–200 km the densities of the main constituents CO_2 in these models are close to the CO_2 density in the recent model of martian neutral atmosphere (midnight, equator) constructed by Bougher *et al.*[18] specially for the period of PHOBOS-2 measurements. The last model presents the information only for two gases.

To calculate the primary photoelectron production rates we employed Hinteregger's AE R74113 EUV reference spectrum as given by Torr and Torr[19]. This solar flux is scaled to Mars' heliocentric distance. The photoabsorption and photoionization cross-sections for N_2, O_2 and O were taken from the work of Torr and Torr[19]. The photoabsorption cross-sections of CO_2 for $\lambda \geq 990$ Å and in the range 480–600 Å were taken from Cairns and Samson[20] and in the range 600–797 Å from Cook *et al.*[21]. In the wavelength range 180–480 Å we adopted the cross-sections measured by Lee *et al.*[22]. The photoionization cross-sections in the wavelength range 600–900 Å were taken from McCulloh[23] and Cook *et al.*[21]. For shorter wavelengths we assumed

a

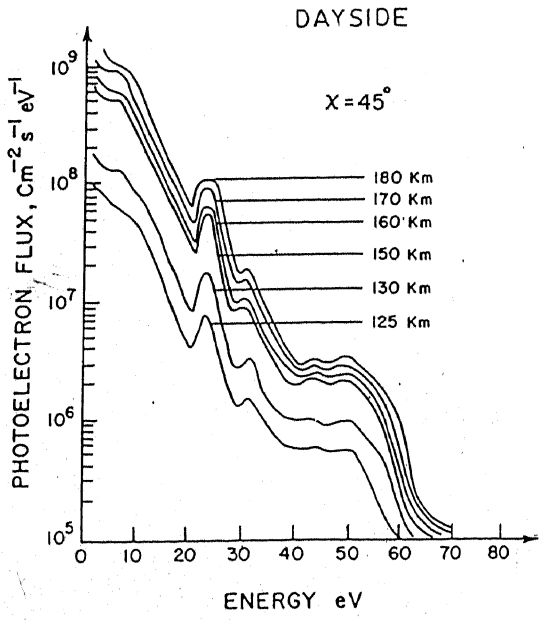

b

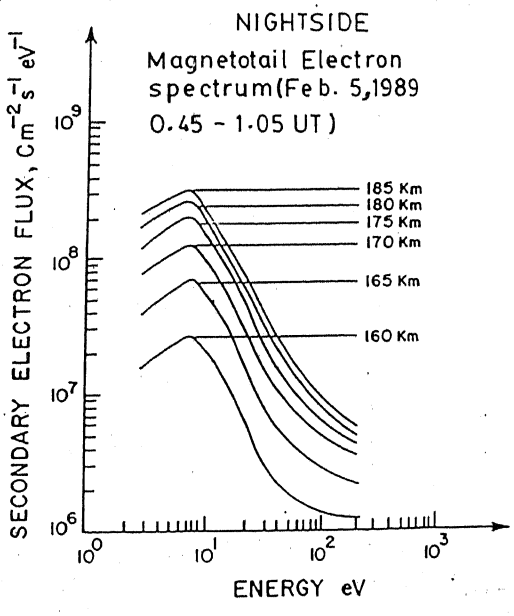

Figure 2. *a* and *b*, Photoelectron and secondary electron fluxes at selected altitudes.

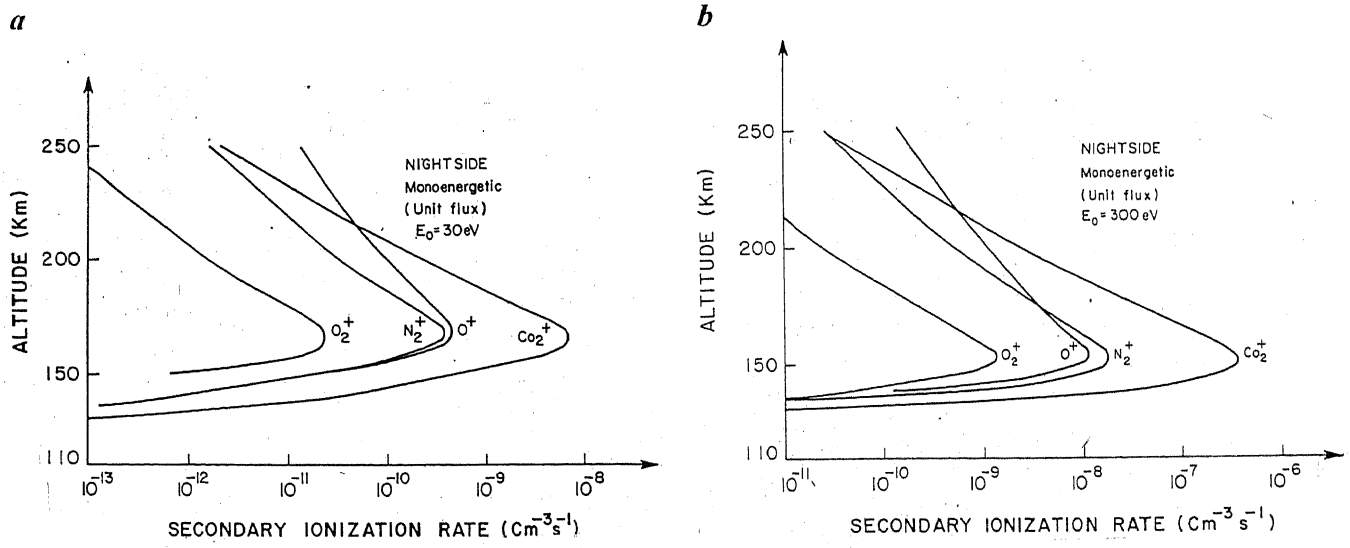

Figure 3. *a*, Secondary ion production rates for E0 = 30 eV for monoenergetic (unit flux) in nighttime ionosphere. *b*, Same as in Figure *a* but for E0 = 300 eV

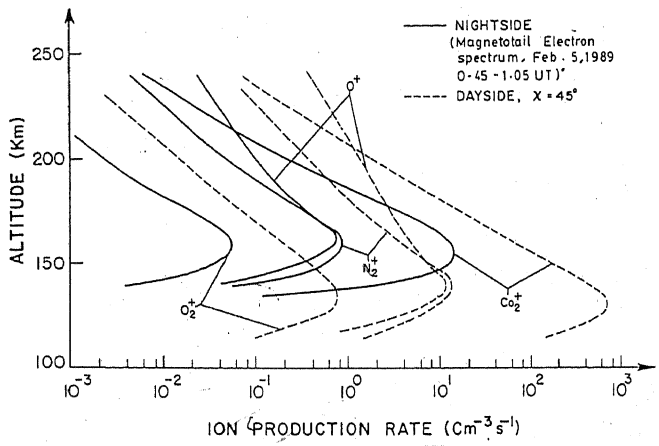

Figure 4. Secondary ion production rates for nighttime and daytime. The solid line shows the calculation for nighttime ionosphere using observed electron spectra. The dashed line shows calculation for daytime at $\chi = 45°$.

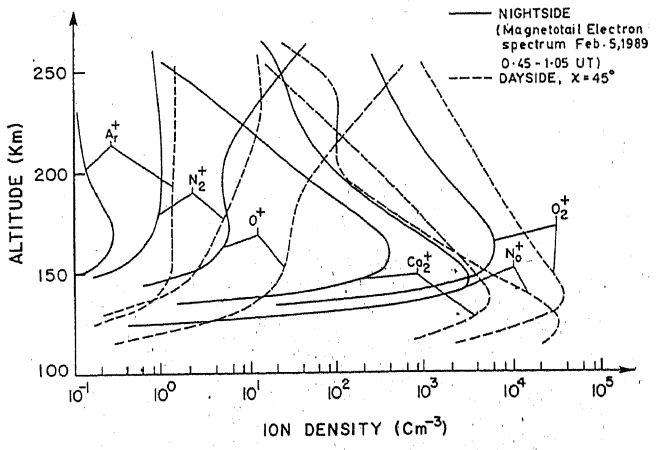

Figure 5. Ion density for nighttime and daytime ionosphere. The solid line presents calculation for electron spectra observed by PHOBOS-2/HARP spectrometer. The dashed line shows calculation for daytime at $\chi = 45°$.

photoionization yield equal to 1. Various branching ratios for N_2, O_2 and O were taken from Torr and Torr[19], and for CO_2 from Gustafson *et al.*[24] and Samson *et al.*[25]. The inelastic and elastic cross-sections needed to calculate secondary electron flux were adopted from Jackman *et al.*[26] and Porter and Jump[27]. Ionization cross-sections for N_2^+, O_2^+, O and CO_2^+ were taken from Green and Sawada[28] and Jackman *et al.*[26].

Calculation details

The precipitation of primary electron flux measured by HARP experiment during martian orbiter PHOBOS-2, onto the planetary atmosphere, followed by a variety of collisional processes, will lead also to the production of a secondary electron flux. In this article the analytical yield spectrum (AYS) approach reported earlier[29–32] is used for the calculation of electron fluxes in the martian nightside and dayside atmosphere. The energy dependence of secondary electron fluxes produced by monoenergetic electrons for the nightside ionosphere of Mars was obtained by using the above method extended for Mars. The net flux of secondary electrons as a function of electron energy and height is obtained by integrating monoenergetic electron flux over primary electron energy using observed primary electron spectra. The peaks of secondary electron fluxes in any case fall within a few eV range. Primary photoelectron production rate at solar zenith angle 45° is calculated by using the standard procedure[16, 32–34]. The result of this calculation is shown in Figure 2. To calculate photoelectron fluxes at different altitudes we have used primary photoelectron production rate and again AYS

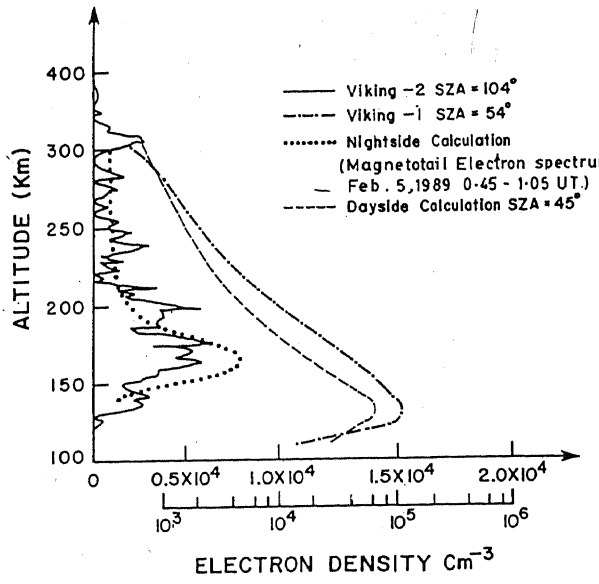

Figure 6. Electron density profiles for nighttime and daytime ionosphere. The solid line shows Viking 2 data at $\chi = 104°$; the dot-dashed line shows daytime electron density profiles observed by Viking 1 at $\chi = 54°$. The dotted line shows nighttime calculation using electron spectra observed by PHOBOS-2/HARP electron experiment. The dashed line shows daytime calculation at $\chi = 45°$.

approach[32, 33]. Figures 2 *a*, *b* show the results of photoelectron and secondary electron flux calculations.

Secondary ionization rates for the nightside and dayside ionosphere of Mars are calculated by using secondary electron flux and photoelectron flux respectively. Figure 4 shows a comparative study of secondary ionization rates for the nightside and dayside ionosphere of Mars. The secondary ionization rates for monoenergetic electrons of unit flux for 30 eV and 300 eV in the nighttime are also calculated. These are shown in Figures 3 *a* and *b*.

For the calculation of the ion densities of different ionic species shown in Figure 5, we have solved the coupled continuity equations for the nightside and dayside ionosphere of Mars by assuming steady-state chemical equilibrium conditions. In this calculation the full set of 18 ionic reactions[17] and their rate coefficients were used. The electron density is obtained by adding the ion densities. The resulting electron densities for the nightside and dayside ionosphere of Mars are plotted in Figure 6.

)n

oelectron production rates at
°0 km, for solar zenith angle
- the calculation
have chosen
eV and
spectral

features in the energy range 20–30 eV are due to the absorption of strong He-II Lyα line at 304 Å. A closer inspection indicates that these features are located at nearly ~ 22–24 eV as indicated by Mantas and Hanson[16] and Fox and Dalgarno[17]. The other major peak which was noted by Mantas and Hanson[16] at ~ 27 eV is not mentioned in the present investigation due to our choice of energy intervals of 2.5 eV above 9 eV. The primary photoelectron energy spectrum falls off by an order of magnitude due to rapid decrease of solar flux and photoionization cross-sections at shorter wavelengths.

Figures 2 *a*, *b* show photoelectron fluxes at 125 km to 180 km for solar zenith angle 45° and secondary electron fluxes at 160 km to 185 km. The peak near 25 eV in photoelectron spectra is due to the peak located in Figure 1 of primary photoelectron production rate. The second peak as noted by Mantas and Hanson[16] is also not found in this calculation due to the same reason as noted for Figure 1. The more structured form of photoelectrons in comparison to secondary electrons in the nighttime is because of more structures in primary photoelectron production rate. Here photoelectron spectra fall by 4 orders of magnitude while in secondary electron spectra in nighttime it falls only by 3 orders of magnitude. This is due to different primary electron spectra taken in the calculation for the nightside and dayside ionosphere of Mars.

Figures 3 *a* and *b* show the secondary ion production rates for CO_2^+, N_2^+, O_2^+ and O^+ for 30 eV and 300 eV using unit flux for the nightside ionosphere of Mars. Figure 4 shows a comparative study of secondary ion production rates for the nightside using observed electron spectra and dayside for solar zenith angle 45°. The peaks of ion CO_2^+ are found at 155 km and 130 km for the nightside and dayside calculation respectively. The ions O_2^+, N_2^+, O^+ peak at ~160 km and ~140 km for nightside and dayside respectively. Therefore, the photoelectron in the dayside lose their energy much deeper in comparison to secondary electrons in the nightside ionosphere of Mars.

Figure 5 presents ion density calculation of Ar^+, N_2^+, O^+, CO_2^+, O_2^+ and NO^+ for the nightside using observed electron spectrum and dayside ionosphere of Mars. In Figures 3 *a*, *b* and 4 the major ion produced is CO_2^+, but it is quickly removed by reactions

$$CO_2^+ + O \rightarrow CO + O_2^+$$

$$CO_2^+ + O \rightarrow O^+ + CO_2$$

$$O^+ + CO_2 \rightarrow CO + O_2^+$$

leading to O_2^+. Therefore, for both nightside and dayside ionospheric studies we find that major ion is O_2^+. The reaction with atomic oxygen is the dominant loss mechanism. The N_2^+, NO^+ and Ar^+ shown in Figure 5

were not detected by Viking experiment. But the N_2^+ and NO^+ ions may be important intermediaries in the escape of nitrogen from the planet[35]. Fox and Dalgarno[17] have noted that above 220 km diffusion becomes more important. In the present calculation we have neglected diffusion completely. Therefore, the peaks of O^+ concentrations disappear in our calculations. The calculated ion compositions of the nightside ionosphere resemble much that of the dayside ionosphere. In daytime in the vicinity of the peak, the second important ion is CO_2^+ while in the nighttime the second important ion is NO^+.

Finally, in Figure 6 we have compared our calculated electron density profiles of the dayside and nightside ionosphere of Mars with Viking 1 and 2 data respectively. The nighttime ionosphere measurements during 50 dual frequency radio occultations of Viking 1 and 2 in 1977 were re-evaluated by Zhang *et al.*[12]. According to these data in 40% profiles[13] were sufficient to detect the peak ionization in the martian nightside ionosphere. Here one profile measured by Viking 2 radio occultation experiment in nighttime is shown in Figure 6. For the comparison of dayside ionospheric profiles we have chosen Viking 1 data for solar zenith angle 54°. The peaks of calculated electron density profiles for nightside and dayside ionosphere are found at 160 km and 130 km respectively, showing close agreement with the observations. The solar EUV flux produces the peak of electron density $\sim 10^5$ cm^{-3} at 130 km while precipitating electrons could reach only the heights of ~160 km and produce electron density 5×10^3. Therefore, dayside electron density is 20 times larger than that of nighttime.

Conclusion

A detailed model calculation of electron fluxes, ion production rates, ion and electron densities has been carried out for the nighttime and daytime ionosphere of Mars. In the present comparative study we find that dayside ionospheric layer is 30 km lower in comparison to nighttime ionosphere of Mars.

The electron spectra in the nighttime atmosphere are less structured in comparison to dayside photoelectron flux spectra. The calculated ion compositions of the nightside ionosphere of Mars much resemble that of dayside ionic compositions. O_2^+ ion density is dominant in both nightside and dayside ionic compositions. The electron spectra observed by HARP experiment in the vicinity of Mars during the second elliptical orbit of PHOBOS 2 show that nighttime ionospheric peak, in any case, should appear at ~160 km.

1. Kliore, A. J., Cain, D. L., Levy, G. S., Eshleman, V. R., Fjeldbo, G. and Drake, F. D., *Science*, 1965, **149**, 1243–1248.
2. Fjeldbo, G., Fjeldbo, W. C. and Eshleman, V. R., *Science*, 1966, **153**, 1515–1523.
3. Fjeldbo, G., Kliore, A. and Seidel, B., *Radio Sci.*, 1970, **5**, 381–386.
4. Kolosov, M. A., Yakovlev, I. O., Kruglov, M. Yo., Trusov, B. P., Efimov, A. I. and Kerzhanovich, V. V., *Radio Eng. Electron. Phys. (USSR)*, 1972, **17**, 1993–1999.
5. Kolosov, M. A., Savich, N. A., Azarkh, S. L., Aleksandrov, N. Yu., Vasiliev, M. B., Vyshlov, A. S., Dubrovin, V. M., Onishehenko, L. V., Somaznaev, I. N., Sidorenko, A. I. and Sorokin, V. P., *Radio Eng. Electron. Phys. (USSR)*, 1973, **18**, 1471–1474.
6. Kliore, A. J., Cain, D. L., Fjeldbo, G., Seidel, B. L., Sykes, M. J. and Rasool, S. I., *Icarus*, 1972, **17**, 484–515.
7. Kliore, A. J., Fjeldbo, G., Seidel, B. L., Sykes, M. J. and Woiceshyn, P. M., *J. Geophys. Res.*, 1973, **78**, 4331–4351.
8. Vasiliev, M. B., Vyshlov, A. S., Kolosov, M. A., Savich, N. A., Samovol, V. A., Samoznayev, L. N., Sidorenko, A. I., Alexandrov, Yu. N., Danilenko, A. I., Dubrovin, V. M., Zarisev, A. L., Petrov, G. M., Rzhiga, O. N., Shern, D. Ya. and Romanova, L. I., *Cosmic Res.*, 1975, **13**, 48–53.
9. Savich, N. A. and Samovol, V. A., *Space Research XVI* (Ed. Rycroft, M. J.), Academie Verlag, Berlin, Germany, 1976, pp. 1009–1010.
10. Fjeldbo, G., Sweetnam, D., Brenkle, J., Christensen, E., Farless, D., Mehta, J., Seidel, B., Michael, W., Wallio, A. and Grossi, M., *J. Geophys. Res.*, 1977, **82**, 4317–4324.
11. Lindal, C. F., Hotz, H. B., Sweetnam, D. W., Shippony, Z., Brenkle, J. P., Hartsell, J. V., Spear, R. T. and Michael, W. M., *J. Geophys. Res.*, 1979, **84**, 8443–8456.
12. Zhang, M. H., Luhman, L. G. and Kliore, A. J., *J. Geophys. Res.*, 1990, **95**, 17095–18003.
13. Verigin, M. I., Gringauz, K. I., Shutte, N. M., Haider, S. A., Szego, K., Kiraly, P., Nagy, A. F. and Gombosi, T. I., *J. Geophys. Res.*, 1991, **96**, 19307–19313.
14. Haider, S. A., Kim, J., Nagy, A. F., Keller, C. N., Verigin, M. I., Gringauz, K. I., Shutte, N. M., Szego, K. and Kiraly, P., *J. Geophys. Res.*, 1991, **97**, 10637–10641.
15. Shutte, N. M., Kiraly, P., Cravens, T. E., Dyachkov, A. V., Gombosi, T. I., Gringauz, K. I., Nagy, A. F., Sharp, W. E., Sheronova, S. M., Toth, A. and Verigin, M. I., *Nature*, 1989, **34**, 614–616.
16. Mantas, G. P. and Hanson, W. B., *J. Geophys. Res.*, 1979, **84**, 369–385.
17. Fox, J. L. and Dalgarno, A., *J. Geophys. Res.*, 1979, **84**, 7315–7333.
18. Bougher, S. W., Dickinson, R. E., Roble, R. G. and Ridley, E. C., *Geophys. Res. Lett.*, 1988, **15**, 1511–1514.
19. Torr, D. G. and Torr, M. R., *J. Atmos. Terr. Phys.*, 1979, **41**, 797–839.
20. Cairns, R. B. and Samson, J. A. R., *J. Geophys. Res.*, 1965, **70**, 99–104.
21. Cook, G. R., Metzger, P. H. and Ogawa, M., *J. Chem. Phys.*, 1966, **44**, 2935–2942.
22. Lee, L. C., Carlson, R. W., Judge, D. L. and Ogawa, M., *J. Quant. Spectrosc. Radiat. Transfer*, 1973, **13**, 1023–1031.
23. McCulloh, K. E., *J. Chem. Phys.*, 1973, **59**, 4252–4259.
24. Gustafson, T., Plummer, E. W., Eastman, D. E. and Gudat, W., *Phys. Rev.*, 1978, **A17**, 175–181.
25. Samson, J. A. R. and Gardner, J. L., *J. Geophys. Res.*, 1973, **78**, 3363–3367.
26. Jackman, C. H., Garvey, R. H. and Green, A. E. S., *J. Geophys. Res.*, 1977, **82**, 5081–5090.
27. Porter, H. S. and Jump, F. W., Tech. Rep., Space Flight Centre, Computer Sci. Greenbelt, MD, USA, 1978.
28. Green, A. E. S. and Sawada, T., *J. Geophys. Res.*, 1972, **34**, 1719–1728.
29. Jackman, C. H. and Green, A. E. S., *J. Geophys. Res.*, 1979, **84**, 2715–2724.
30. Green, A. E. S. and Singhal, R. P., *Geophys. Res. Lett.*, 1979, **6**, 625–628.

31. Haider, S. A. and Singhal, R. P., *J. Geophys. Res.*, 1983, **88**, 7185–7189.
32. Singhal, R. P. and Haider, S. A., *J. Geophys. Res.*, 1984, **89**, 6847–6852.
33. Haider, S. A., *J. Geophys. Res.*, 1986, *91*, 8998–9000.
34. Bhardwaj, A., Haider, S. A. and Singhal, R. P., *Icarus*, 1990, **85**, 216–228.
35. Yung, Y. L., Strobel, D. F., Kong, T. Y. and McELroy, M. B., *Icarus*, 1977, **30**, 26–41.

ACKNOWLEDGEMENT. I thank Prof. B. H. Subbaraya for his valuable suggestions and discussions.